THE JOURNAL OF PHYSICAL CHEMISTRY B

Article

pubs.acs.org/JPCB

Alkylimidazolium Based Ionic Liquids: Impact of Cation Symmetry on Their Nanoscale Structural Organization

Marisa A. A. Rocha,[†] Catarina M. S. S. Neves,[‡] Mara G. Freire,[‡] Olga Russina,[§] Alessandro Triolo,[∥] João A. P. Coutinho,*[,‡] and Luís M. N. B. F. Santos*[,†]

[†]Centro de Investigação em Química, Departamento de Química e Bioquímica, Faculdade de Ciências, Universidade do Porto, R. Campo Alegre 687, P-4169-007 Porto, Portugal

[‡]Departamento de Química, CICECO, Universidade de Aveiro, P-3810-193 Aveiro, Portugal

[§]Department of Chemistry, University of Rome "Sapienza", Piazzale Aldo Moro 5, I-00185 Rome, Italy

[∥]Istituto di Struttura della Materia, Consiglio Nazionale delle Ricerche, Via del Fosso del Cavaliere 100, I-00133 Rome, Italy

Supporting Information

ABSTRACT: Aiming at evaluating the impact of the cation symmetry on the nanostructuration of ionic liquids (ILs), in this work, densities and viscosities as a function of temperature and small−wide angle X-ray scattering (SWAXS) patterns at ambient conditions were determined and analyzed for 1-alkyl-3-methylimidazolium bis(trifluoromethylsulfonyl)imide (asymmetric) and 1,3-dialkylimidazolium bis-(trifluoromethylsulfonyl)imide (symmetric) series of ionic liquids. The symmetric IL series, $[C_{N/2}C_{N/2}im][NTf_2]$, presents lower viscosities than the asymmetric $[C_{N-1}C_1im][NTf_2]$ counterparts. For ionic liquids from $[C_1C_1im][NTf_2]$ to $[C_6C_6im][NTf_2]$, an odd−even effect in the viscosity along the cation alkyl side chain length was observed, in contrast with a linear increase found for the ones ranging between $[C_6C_6im][NTf_2]$ and $[C_{10}C_{10}im][NTf_2]$. The analysis of the viscosity data along the alkyl side chain length reveals a trend shift that occurs at $[C_6C_1im][NTf_2]$ for the asymmetric series and at $[C_6C_6im][NTf_2]$ for the symmetric series. These results are further supported by SWAXS measurements at ambient conditions. The gathered data indicate that both asymmetric and symmetric members are characterized by the occurrence of a distinct degree of mesoscopic structural organization above a given threshold in the side alkyl chain length, regardless the cation symmetry. The data also highlight a difference in the alkyl chain dependence of the mesoscopic cluster sizes for symmetric and asymmetric cations, reflecting a different degree of interdigitation of the aliphatic tails in the two families. The trend shift found in this work is related to the structural segregation in the liquid after a critical alkyl length size (CALS) is attained and has particular relevance in the cation structural isomerism with higher symmetry.

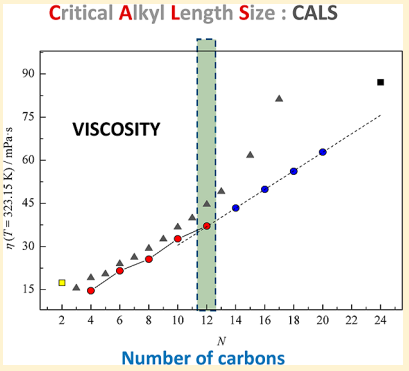

1. INTRODUCTION

The physical properties of ionic liquids (ILs) depend on the nature, size, and shape of both their cations and anions. Therefore, the properties of ILs can be tuned over a wide range by adjusting the structure and chemical composition of the constituting ions. This tunability feature, achieved with the high number of possible ILs that can be formed by combining different cation and anion pairs, by introducing isomerization effects and variations in the alkyl side chains, has made of ILs a focus of intensive research.[1,2] Some ILs can be considered as nanostructurated fluids in which the ion pairs arrange themselves into polar and nonpolar domains. It is the interplay of these two domains/interactions that eventually leads to the formation of medium-range nanoscale domains. This was first recognized by computer simulations studies[3,4] and then confirmed experimentally.[5−7] It was later shown, by molecular dynamics (MD) simulation, that the structural segregation in ILs depends on the size of the polar and nonpolar regions in which each ion may exist as dispersed or continuous microphases.[8,9] On the basis of these works[8,9] it was possible to detect that the transition between these two phases depends on the relative size of the high-charge and low-charge regions in each ion and on the size of the aliphatic moiety. These findings were later experimentally confirmed by a thermodynamic study concerning the vaporization of an extended series of ILs, $[C_{N-1}C_1im][NTf_2]$, where it was found, for the first time, that their thermodynamic properties of vaporization and their heat capacities present trend shifts along the studied series, which are related to a change in the molecular structure of the liquid for compounds larger than $[C_6C_1im][NTf_2]$.[10,11]

Additionally, the cation symmetry provides a different structural organization which also allows the fine-tuning of IL's physicochemical properties. Dzyuba and Bartsch[12] showed that the $[C_{N/2}C_{N/2}im][PF_6]$, with N = 8, 10, 14, 16, 18, and 20,

Received: June 27, 2013
Revised: August 5, 2013
Published: August 5, 2013

present melting temperatures below 373 K. These results demonstrated that one important factor that determines the low melting points of ILs is the asymmetric nature of the cation. Xiao et al.,[13] based on small−wide angle X-ray scattering (SWAXS) data and optical Kerr effect (OKE) spectra, showed that the symmetric IL series, $[C_{N/2}C_{N/2}im][NTf_2]$, presents higher local order and higher intermolecular dynamics in frequency than the asymmetric series, $[C_{N-1}C_1im][NTf_2]$. SWAXS measurements provide information related to the structural heterogeneities in ILs, and on the basis of the data gathered by this technique, Zheng et al.[14] found that, for the asymmetric imidazolium-based ILs, the structural heterogeneities extend over a large spatial scale when compared with the symmetric ILs. In the same work,[14] the authors observed that the densities for a symmetric/asymmetric IL pair, with a given total number of carbons, are similar and the viscosity of the asymmetric ILs is larger than that found for the symmetric fluids. Also, it was observed an odd−even effect on the viscosity data similar to what is found in simulations of ion diffusion coefficients.[14] A recent atomistic MD simulation[15] study and coarse grained molecular dynamics (CG-MD)[16] from the group of Balasubramanian focused on the exploration of mesoscopic order in symmetric imidazolium cations. The authors[15,16] studied symmetric and asymmetric cations with relatively short alkyl chains (the same ILs experimentally investigated by Xiao and co-workers[13]) with N = 4−6 and the bistriflamide anion. This study[15,16] essentially confirmed the structural scenario observed experimentally, providing atomistic inspection into the morphological properties of these systems, by mimicking the experimental data. The authors have also previously investigated the IL 1,3-didecylimidazolium hexafluorophosphate that, although bearing a different anion with respect to the ones for which experimental data are available, is characterized by the cation bearing two relatively long decyl chains. In this case the authors observed a peculiar structural behavior as the sample turned out to be characterized by a pseudolamellar structural organization.

Recently, Rocha et al.[17] assessed the effect of the cation topological symmetry on the thermodynamic properties of vaporization for the symmetric $[C_{N/2}C_{N/2}im][NTf_2]$ ILs, with N = 4, 6, 8, 10, and 12. It was found that the symmetric imidazolium-based ILs present a higher volatility than the asymmetric counterparts, $[C_{N-1}C_1im][NTf_2]$. The obtained vaporization results showed an enthalpic and entropic differentiation with a clearly discernible odd−even effect, with higher enthalpies and entropies of vaporization for the odd-numbered ILs, and in agreement with the trend observed by Zheng et al.[14]

Tariq et al.[18,19] explored the effect of temperature, cation alkyl side chain length, and cation and anion nature on a systematic study of densities, viscosities, surface tensions, and refractive indices in order to obtain some insights on the intermolecular forces and behavior in solutions of different ILs. The authors[18,19] suggested that the structural segregation in ILs does not affect, or at most it has a negligible effect on, the trends found for the volumetric behavior, in terms of both temperature and alkyl side chain length. However, based on the reanalysis of the viscosity data published by Tariq et al.[19] for the series of the $[C_{N-1}C_1im][NTf_2]$ ILs, Rocha et al.[10] have shown the existence of two regions in the viscosity dependency of the alkyl chain, and could relate it to the structural segregation occurring in longer alkyl chain ILs.

On the basis of all the described scenarios and aiming at evaluating the impact of the cation symmetry on the nanostructuration of ILs, in the present work, the densities and viscosities, and their dependence on temperature, of 1,3-dialkylimidazolium bis(trifluoromethylsulfonyl)imide, $[C_{N/2}C_{N/2}im][NTf_2]$, are compared to those of 1-alkyl-3-methylimidazolium bis(trifluoromethylsulfonyl)imide, $[C_{N-1}C_1im][NTf_2]$, for a wide set of N values. Moreover, SWAXS data have been collected at ambient temperature for the same group of fluids. The combined approaches were then used to properly evaluate the influence of the structural segregation of ILs as well as the symmetry effect on their thermophysical properties. The schematic representation of the studied ILs is presented in Figure 1.

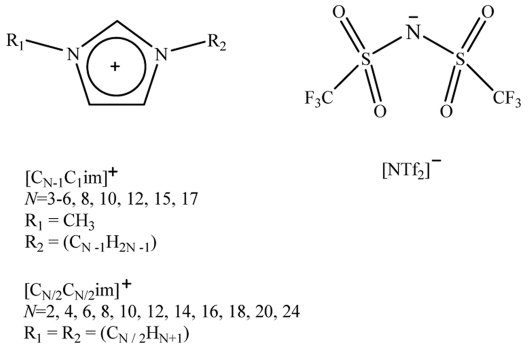

Figure 1. Schematic representation of the imidazolium based ionic liquids, where N corresponds to the total number of carbons in the two alkyl side chains in the cation. υ, number of alkyl groups in the longest chain that is either $\upsilon = N - 1$ in the case of asymmetric or $\upsilon = N/2$ in the case of symmetric.

2. EXPERIMENTAL SECTION

2.1. Materials. The densities, viscosities, and small−wide angle X-ray scattering (SWAXS) spectra were measured for the following imidazolium-based ionic liquids: 1-alkyl-3-methylimidazolium bis(trifluoromethylsulfonyl)imide, $[C_{N-1}C_1im][NTf_2]$ (with N = 3−6, 8, 10, 12, 15, 17), and 1,3-dialkylimidazolium bis(trifluoromethylsulfonyl)imide, $[C_{N/2}C_{N/2}im][NTf_2]$ (with N = 2−20, 24). All ILs were purchased from Iolitec. Before the measurements, the ionic liquids were dried and purified under high vacuum (10^{-3} Pa) and at moderate temperature (353 K) for at least 48 h. The purity of each ionic liquid was further evaluated by ^{1}H, ^{13}C, and ^{19}F NMR spectra, and all samples found to be >99 wt % pure. The water mass fraction contents were determined with a Metrohm 831 Karl Fischer coulometer, using a Hydranal-Coulomat AG from Riedel-de Haën. The water content, in all samples, was below 100 ppm.

2.2. Densities and Viscosities. Density and viscosity measurements for the pure ionic liquids were performed at atmospheric pressure in the temperature range from 278.15 to 363.15 K. Only for $[C_{14}C_1im][NTf_2]$, $[C_{16}C_1im][NTf_2]$, $[C_1C_1im][NTf_2]$, and $[C_{12}C_{12}im][NTf_2]$ were the measurements performed in a narrower temperature range since these compounds are solid at room temperature. The measurements were carried out using an automated SVM 3000 Anton Paar rotational Stabinger viscometer−densimeter, and the detailed description concerning the operation of the system, calibration, and validation is described elsewhere.[20] The SVM 3000 uses Peltier elements for fast and efficient thermostability, where the uncertainty in temperature is within ±0.02 K. The apparatus was calibrated by measuring the viscosity/density of three

Table 1. Fitting Parameters of eq 1 and Thermal Expansion Coefficients, α_p, at 323.15 K and 0.1 MPa for the Studied Ionic Liquids

ionic liquid	a	$(10^4 \times b)/K^{-1}$	$(10^7 \times c)/K^{-2}$	$(10^3 \times \alpha_p(T=323.15\ K))/K^{-1}$
		$[C_{N-1}C_1im][NTf_2]$		
$[C_2C_1im][NTf_2]$	7.5304 ± 0.0010	−7.004 ± 0.064	0.49 ± 0.10	0.669 ± 0.009
$[C_3C_1im][NTf_2]$	7.5029 ± 0.0010	−7.098 ± 0.066	0.60 ± 0.10	0.671 ± 0.009
$[C_4C_1im][NTf_2]$	7.4734 ± 0.0013	−7.125 ± 0.084	0.70 ± 0.13	0.667 ± 0.012
$[C_5C_1im][NTf_2]$	7.4570 ± 0.0010	−7.384 ± 0.061	1.099 ± 0.096	0.667 ± 0.009
$[C_7C_1im][NTf_2]$	7.4059 ± 0.0018	−6.83 ± 0.11	0.17 ± 0.18	0.672 ± 0.016
$[C_9C_1im][NTf_2]$	7.3787 ± 0.0014	−7.310 ± 0.090	0.92 ± 0.14	0.672 ± 0.013
$[C_{11}C_1im][NTf_2]$	7.3524 ± 0.0013	−7.417 ± 0.080	0.99 ± 0.12	0.678 ± 0.011
$[C_{14}C_1im][NTf_2]$	7.3274 ± 0.0064	−8.20 ± 0.37	2.03 ± 0.54	0.689 ± 0.051
$[C_{16}C_1im][NTf_2]$	7.3114 ± 0.0049	−8.30 ± 0.29	2.06 ± 0.41	0.697 ± 0.039
		$[C_{N/2}C_{N/2}im][NTf_2]$		
$[C_1C_1im][NTf_2]$	7.5675 ± 0.0013	−7.344 ± 0.078	1.10 ± 0.12	0.663 ± 0.011
$[C_2C_2im][NTf_2]$	7.5010 ± 0.0009	−6.970 ± 0.053	0.348 ± 0.082	0.675 ± 0.007
$[C_3C_3im][NTf_2]$	7.4571 ± 0.0010	−7.518 ± 0.065	1.19 ± 0.10	0.675 ± 0.009
$[C_4C_4im][NTf_2]$	7.4157 ± 0.0010	−7.530 ± 0.066	1.27 ± 0.10	0.671 ± 0.009
$[C_5C_5im][NTf_2]$	7.3750 ± 0.0009	−7.338 ± 0.058	0.907 ± 0.090	0.675 ± 0.008
$[C_6C_6im][NTf_2]$	7.3487 ± 0.0016	−7.49 ± 0.10	1.07 ± 0.15	0.680 ± 0.014
$[C_7C_7im][NTf_2]$	7.3216 ± 0.0016	−7.322 ± 0.097	0.86 ± 0.15	0.677 ± 0.014
$[C_8C_8im][NTf_2]$	7.2979 ± 0.0017	−7.36 ± 0.11	0.81 ± 0.16	0.684 ± 0.015
$[C_9C_9im][NTf_2]$	7.2761 ± 0.0024	−7.35 ± 0.15	0.79 ± 0.23	0.684 ± 0.021
$[C_{10}C_{10}im][NTf_2]$	7.2666 ± 0.0016	−7.63 ± 0.10	1.17 ± 0.15	0.687 ± 0.014
$[C_{12}C_{12}im][NTf_2]$	7.2361 ± 0.0070	−7.69 ± 0.41	1.28 ± 0.59	0.686 ± 0.056

Anton Paar standard calibration samples, APN7.5, APN26, and APN415, in steps of 5 K in the temperature range from 293.15 to 393.15 K. The reproducibility of the dynamic viscosity and density measurements is in accordance to the levels given by the manufacturer, namely ±0.35% and ±0.5 kg·m^{-3}, from 288.15 to 378.15 K.

2.3. Small−Wide Angle X-ray Scattering. SWAXS data were collected at the ID15b beamline at the ESRF synchrotron in Grenoble, using an instrumental setup that covers a wide momentum transfer range (namely, using a monochromatic beam with energy of 60 keV, one can access from 0.2 to ca. 20 Å^{-1}). Measurements were performed using a thermostat, maintaining the temperature at 298.15 K, and the samples were kept in a quartz capillary with an outer diameter of 2 mm. The corresponding empty cell contribution was subtracted. In the present paper we focus attention on the low Q portion of the data sets, limiting the range from 0.2 to 1.7 Å^{-1}. Measurements were also performed at the SWAXS beamline ID02 at ESRF (Grenoble), aiming to cover the lower Q range (0.03−1.2 Å^{-1}), using a monochromatic beam with energy of 19.8 keV and the same sample environment.

3. RESULTS AND DISCUSSION

3.1. Densities. Densities for pure ionic liquids were determined at atmospheric pressure and in the temperature range from 278.15 to 363.15 K, with the exception of $[C_{14}C_1im][NTf_2]$, $[C_{16}C_1im][NTf_2]$, $[C_1C_1im][NTf_2]$, and $[C_{12}C_{12}im][NTf_2]$ that display melting temperatures higher than room temperature. The experimental densities of the studied compounds are reported in Tables 1S and 2S as Supporting Information. The experimental density data (ρ), in the studied temperature (T) range, was further correlated using the second order polynomial equation:

$$\ln(\rho) = a + bT + cT^2 \quad (1)$$

where a, b, and c are constants obtained from the fitting. The graphic representation of the logarithm of density as a function of temperature and the respective relative deviations between the experimental density measured in this work and those reported in the literature[14,18,21−25] are presented as Supporting Information. The experimental density data gathered in this work are in good agreement with literature results showing deviations on the order of 0.2% for the majority of the studied ionic liquids. Two exceptions were observed for $[C_4C_1im][NTf_2]$[21,23] and $[C_2C_1im][NTf_2]$,[18] where significantly larger deviations were found. These higher deviations could be related to the IL sample purity (such as water content), deficiencies in the experimental methodologies, and lower apparatus accuracy.

The isobaric thermal expansion coefficient, α_p, which considers the volumetric changes with temperature, was calculated using eq 2:

$$\alpha_p = -\frac{1}{\rho}\left(\frac{\partial \rho}{\partial T}\right)_p = -\left(\frac{\partial \ln \rho}{\partial T}\right)_p = -(b + 2cT) \quad (2)$$

where ρ is the density in kg·m^{-3}, T is the temperature in K, and p is the standard pressure (10^5 Pa), while b and c are the fitting parameters of eq 1. Furthermore, based on the propagation of errors from the standard deviations coupled to each parameter adjustment, very small, i.e., no statistically significant, temperature dependence can be assigned to α_p. Table 1 lists the fitting parameters of eq 1 and the thermal expansion coefficients, at 323.15 K and 0.1 MPa, for all the investigated ionic liquids. The graphic representations of the density and thermal expansion coefficients, at 323.15 K and 0.1 MPa, as a function of the total number of carbons of the alkyl side chains length, N, are depicted in Figure 2. Due to the fact that some of the studied ionic liquids are solid at 298.15 K, the comparison between the two studied families is presented at T = 323.15 K.

Above N = 6 and for the same total number of carbons in the alkyl chains, the symmetric series seems to present a somewhat lower density than the asymmetric ones. The explanation of

dx.doi.org/10.1021/jp406374a | J. Phys. Chem. B 2013, 117, 10889−10897

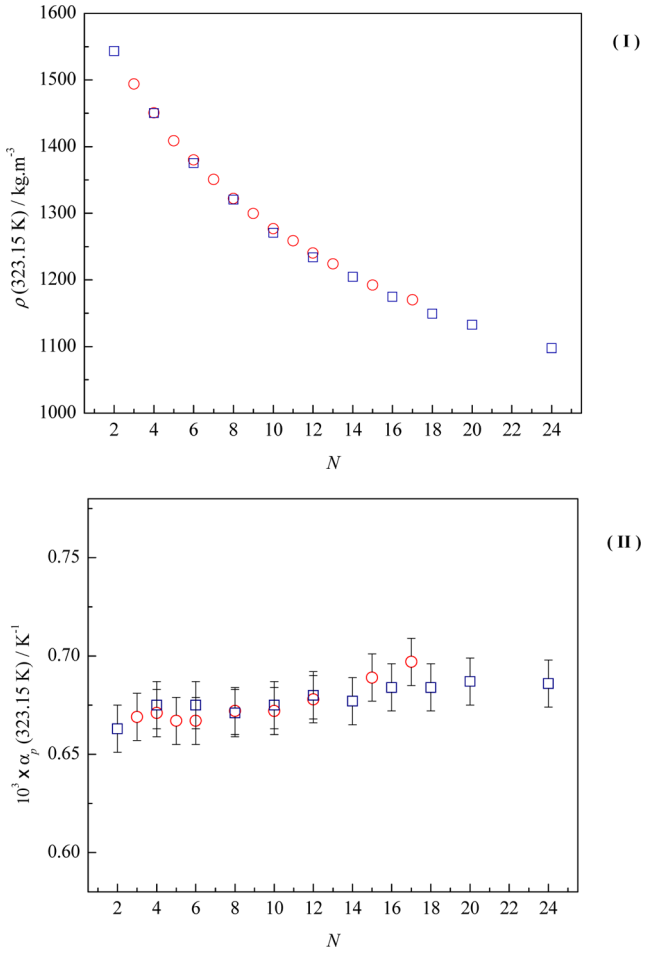

Figure 2. Graphic representation of the (I) density and (II) thermal expansion coefficient, at 323.15 K and 0.1 MPa, as a function of the total number of carbons of the alkyl side chain length, *N*. Red open circles, $[C_{N-1}C_1im][NTf_2]$; blue open squares, $[C_{N/2}C_{N/2}im][NTf_2]$.

that subtle difference is, in our opinion, quite challenging due to the small differentiation of the data. Concerning the thermal expansion coefficients, they are very similar, increasing only slightly with the alkyl chain length from 6.6×10^{-4} K^{-1} for $[C_1C_1im][NTf_2]$ to 7.0×10^{-4} K^{-1} for $[C_{16}C_1im][NTf_2]$. No significant differentiation could be detected in the thermal expansion coefficients between the asymmetry and symmetric IL series.

3.2. Viscosities. The experimental viscosity data (η) for the studied ionic liquids are reported in Tables 3S and 4S in the Supporting Information, and the graphic representations of ln(η/mPa·s) against the temperature and the deviations between the experimental viscosity measured in this work and those reported in the literature[14,19,25] are presented in Figures 3S and 4S in the Supporting Information. The experimental viscosity data for the $[C_{N-1}C_1im][NTf_2]$ series are in good agreement with the literature data, within 1%, with the exception of $[C_5C_1im][NTf_2]$,[19] which presents a relative deviation on the order of 8%. The higher positive deviation observed with this ionic liquid could be related to the higher water content which thus leads to a significant decrease in viscosity. In the case of the $[C_{N/2}C_{N/2}im][NTf_2]$ ionic liquids, the data presented for $[C_4C_4im][NTf_2]$ are in excellent agreement with the literature data.[25]

The data published previously by Zheng et al.[14] present a deviation of ±15% from our results, which indicates a systematic deviation in their viscosity sensitivity coefficient that could arise from the procedure used in the apparatus calibration based on a single viscosity standard. The experimental viscosity data were correlated using the Vogel–Tammann–Fulcher (VTF) model described in eq 3:

$$\eta(T) = A_\eta \exp\left[\frac{B_\eta}{T - C_\eta}\right] \quad (3)$$

where $\eta(T)$ is the viscosity in mPa·s, T is the temperature in K, and A_η, B_η, and C_η are adjustable parameters. The adjustable parameters were determined from the fitting of the experimental data using eq 3. The derived coefficients of the VTF equation are presented in Table 2. The correlated viscosities are in good agreement with the experimental data. For the studied ionic liquids a maximum relative deviation of 1% for the correlated values was achieved. Some of the data were already available in the literature[19] and are here used in the discussion/analysis aiming for better understanding of the results and related accuracy obtained in this work.

The viscosity describes the internal resistance of a fluid to a shear stress, and as is well-known, ionic liquids show higher viscosities than common molecular solvents show. The ionic liquid high viscosities are a direct consequence of their high molecular weights as well as their multiple intermolecular interactions (H-bonding, dispersive and electrostatic interactions). As the viscosity arises from intermolecular interactions, an increase in temperature will substantially decrease their intensity and therefore the viscosity. The energy barrier of the fluid to a shear stress, E, can be evaluated based on the viscosity dependence with the temperature using the following equation:

$$E = R\,\frac{\partial(\ln[\eta(T)])}{\partial(1/T)} = R\left(\frac{B_\eta}{\frac{C_\eta^{\,2}}{T^2} - \frac{2C_\eta}{T} + 1}\right) \quad (4)$$

The derived energy barrier, E, at T = 323.15 K, is listed in Table 2. The graphic representations of the viscosity and energy barrier at 323.15 K, and the pre-exponential coefficient, A_η, of the VTF equation as a function of the total number of carbon atoms in the alkyl chains of the cation, are presented in Figures 3 and 4.

As previously shown by us for other properties,[10,11,17] in Figures 3I and 4I there is a shift in the viscosity trend above $[C_6C_1im][NTf_2]$ for the asymmetric series and $[C_6C_6im]$-$[NTf_2]$ for the symmetric ILs. This trend shift is related to the structural organization of the liquid above a critical alkyl length size, CALS, and that is particularly emphasized by the cation structural isomerism with a higher symmetry for the $[C_{N/2}C_{N/2}im][NTf_2]$ series. In "Region A", in Figure 3I, a subtle but clearly visible odd–even effect for the viscosity with increasing alkyl side chain length was found in asymmetric ionic liquids (from $[C_2C_1im][NTf_2]$ to $[C_6C_1im][NTf_2]$), in contrast with the linear increase for the "Region B" (from $[C_7C_1im][NTf_2]$ to $[C_{12}C_1im][NTf_2]$). Starting from $[C_{12}C_1im][NTf_2]$, the ionic liquids show a progressive positive deviation (toward higher viscosities) from the linear behavior observed in "Region B". The positive deviation for the long alkyl side chain ionic liquids is identical to that observed for the long chain alkane derivatives[27,28] and is related to the increase of the conformational entropy and possibility of alkyl chain

dx.doi.org/10.1021/jp406374a | J. Phys. Chem. B 2013, 117, 10889–10897

Table 2. Fitting Coefficients of the VTF Equation for Viscosity Data of the Studied Ionic Liquids and the Derived Energy Barrier at 323.15 K

ionic liquid	A_η/(mPa·s)	B_η/K	C_η/K	$E(T=323.15\ K)/(kJ\cdot mol^{-1})$
		$[C_{N-1}C_1im][NTf_2]$		
$[C_2C_1im][NTf_2]$	0.215 ± 0.003	709.7 ± 4.0	157.1 ± 0.4	22.35 ± 0.24
$[C_3C_1im][NTf_2]$	0.194 ± 0.001	717.4 ± 1.6	166.8 ± 0.2	25.48 ± 0.15
$[C_4C_1im][NTf_2]$	0.160 ± 0.002	774.2 ± 4.4	163.6 ± 0.4	26.41 ± 0.31
$[C_5C_1im][NTf_2]$	0.156 ± 0.001	790.6 ± 2.0	166.2 ± 0.2	27.87 ± 0.16
$[C_6C_1im][NTf_2]$	0.134 ± 0.001	837.1 ± 2.6	164.6 ± 0.2	28.91 ± 0.17
$[C_7C_1im][NTf_2]$	0.119 ± 0.001	883.5 ± 1.6	162.8 ± 0.1	29.83 ± 0.09
$[C_8C_1im][NTf_2]$	0.113 ± 0.002	908.8 ± 4.5	162.8 ± 0.4	30.69 ± 0.34
$[C_9C_1im][NTf_2]$	0.108 ± 0.003	937.4 ± 7.8	162.4 ± 0.6	31.50 ± 0.54
$[C_{10}C_1im][NTf_2]$	0.096 ± 0.002	978.1 ± 6.8	160.9 ± 0.5	32.26 ± 0.46
$[C_{11}C_1im][NTf_2]$	0.096 ± 0.003	995 ± 10	161.3 ± 0.8	32.99 ± 0.74
$[C_{12}C_1im][NTf_2]$	0.087 ± 0.002	1034.5 ± 7.4	160.0 ± 0.6	33.74 ± 0.55
$[C_{14}C_1im][NTf_2]$	0.092 ± 0.009	1040 ± 34	163.4 ± 2.9	35.4 ± 2.9
$[C_{16}C_1im][NTf_2]$	0.097 ± 0.008	1039 ± 28	168.7 ± 2.3	37.8 ± 2.6
		$[C_{N/2}C_{N/2}im][NTf_2]$		
$[C_1C_1im][NTf_2]$	0.219 ± 0.003	716.7 ± 5.0	159.2 ± 0.6	23.15 ± 0.37
$[C_2C_2im][NTf_2]$	0.148 ± 0.004	821.0 ± 8.8	144.5 ± 0.9	22.33 ± 0.47
$[C_3C_3im][NTf_2]$	0.150 ± 0.001	782.2 ± 1.7	165.8 ± 0.2	27.43 ± 0.16
$[C_4C_4im][NTf_2]$	0.120 ± 0.002	863.9 ± 3.9	162.1 ± 0.3	28.92 ± 0.25
$[C_5C_5im][NTf_2]$	0.095 ± 0.002	948.7 ± 6.7	160.7 ± 0.5	31.21 ± 0.44
$[C_6C_6im][NTf_2]$	0.084 ± 0.002	998.7 ± 8.1	159.4 ± 0.6	32.34 ± 0.54
$[C_7C_7im][NTf_2]$	0.079 ± 0.005	1039 ± 19	158.6 ± 1.4	33.3 ± 1.3
$[C_8C_8im][NTf_2]$	0.067 ± 0.003	1104 ± 15	156.4 ± 1.0	34.47 ± 0.92
$[C_9C_9im][NTf_2]$	0.065 ± 0.002	1127.4 ± 8.1	156.4 ± 0.6	35.20 ± 0.55
$[C_{10}C_{10}im][NTf_2]$	0.079 ± 0.009	1086 ± 37	160.7 ± 2.8	35.7 ± 2.7
$[C_{12}C_{12}im][NTf_2]$	0.0704 ± 0.0003	1153.5 ± 1.4	161.2 ± 0.1	38.19 ± 0.10

folding. This is in agreement also with the higher energy barriers arising from the increase of shear stress.

In Figure 4I, the viscosities at 323.15 K of the symmetric IL series, $[C_{N/2}C_{N/2}im][NTf_2]$, and the asymmetric series, $[C_{N-1}C_1im][NTf_2]$, are compared. It can be observed that the ILs with symmetric cations present a significantly lower viscosity than the asymmetric series present. Moreover, the viscosity results for the $[C_{N/2}C_{N/2}im][NTf_2]$ series show a clearly discernible odd−even effect in "Region A" ($[C_2C_2im][NTf_2]$ to $[C_6C_6im][NTf_2]$), in which the odd-numbered ILs ($[C_3C_3im][NTf_2]$ to $[C_5C_5im][NTf_2]$) present higher viscosities. An odd−even effect was also recently reported for the thermodynamic study of vaporization for the same IL series, where higher enthalpies and entropies of vaporization for the odd-numbered $[C_3C_3im][NTf_2]$ and $[C_5C_5im][NTf_2]$ were found.[17] In "Region B", starting at $[C_7C_7im][NTf_2]$ and going until $[C_{10}C_{10}im][NTf_2]$, the odd−even effect ceases and a linear increase of the viscosity of 3.23 ± 0.03 mPa·s per methylene group, $-CH_2-$, is observed, essentially identical to the increment found for the asymmetric series of 3.6 ± 0.1 mPa·s. As observed for the $[C_{N-1}C_1im][NTf_2]$ series, above $[C_{12}C_1im][NTf_2]$, the viscosity of the ionic liquid $[C_{12}C_{12}im][NTf_2]$ deviates toward higher viscosities from the linear behavior observed in "Region B". The odd−even effect in "Region A" reflects and supports the existence of structuration on the charged region and highlights the effect of the short alkyl chain ILs in that interaction.[17] This effect is related to the predominant orientation of the terminal methyl group of the alkyl chain to the imidazolium ring and their influence in the cation−anion interaction. That phenomenon was also observed recently in the vapor−liquid equilibrium study for the same series[17] and is in qualitative agreement, with higher viscosities associated with higher enthalpies and entropies of vaporization. In Figures 3II and 4II, a fast decrease of the pre-exponential parameter of the VTF equation, A_η, is observed for "Region A", from $[C_3C_1im][NTf_2]$ to $[C_6C_1im][NTf_2]$ (for the asymmetric ILs) and from $[C_2C_2im][NTf_2]$ to $[C_6C_6im][NTf_2]$ (for the symmetric series). The sharp decrease of A_η in "Region A" is related to the decrease of the surface−volume ratio of the ion pair. In "Region B" the decrease of the A_η parameter with increasing chain length is significantly reduced and could be explained by the loss of the sphericity and increasing elongation shape of the ion pair above $[C_6C_1im][NTf_2]$ or $[C_6C_6im][NTf_2]$. The energy barrier at 323.15 K, E, increases monotonically in both IL series, with a faster increase in "Region A" and a linear increase around 1 $kJ\cdot mol^{-1}$ per methylene group in "Region B". This pattern is in qualitative agreement with the trend observed for the enthalpies of vaporization.[10,17] $[C_1C_1im][NTf_2]$ shows the typical and expected outlier behavior, for the viscosity and VTF parameters, relative to the homologues series, with a higher viscosity, higher A_η value, and higher energy barrier, E, than what would be obtained by the extrapolation of the homologues series trend.

3.3. Small−Wide Angle X-ray Scattering. SWAXS data from 1-alkyl-3-methylimidazolium bis(trifluoromethylsulfonyl)-imide, $[C_{N-1}C_1im][NTf_2]$ (with N = 3−13), and 1,3-dialkylimidazolium bis(trifluoromethylsulfonyl) imide, $[C_{N/2}C_{N/2}im][NTf_2]$ (with even members of N = 2−16, 20), are reported in Figure 5. SWAXS results for the asymmetric imidazolium-based ILs have been already reported, but only $[C_{N/2}C_{N/2}im][NTf_2]$ with N = 6, 8, and 10 have been studied so far.[13,14] Therefore, in the present work we present new findings using SWAXS data for the extended series of the

dx.doi.org/10.1021/jp406374a | J. Phys. Chem. B 2013, 117, 10889−10897

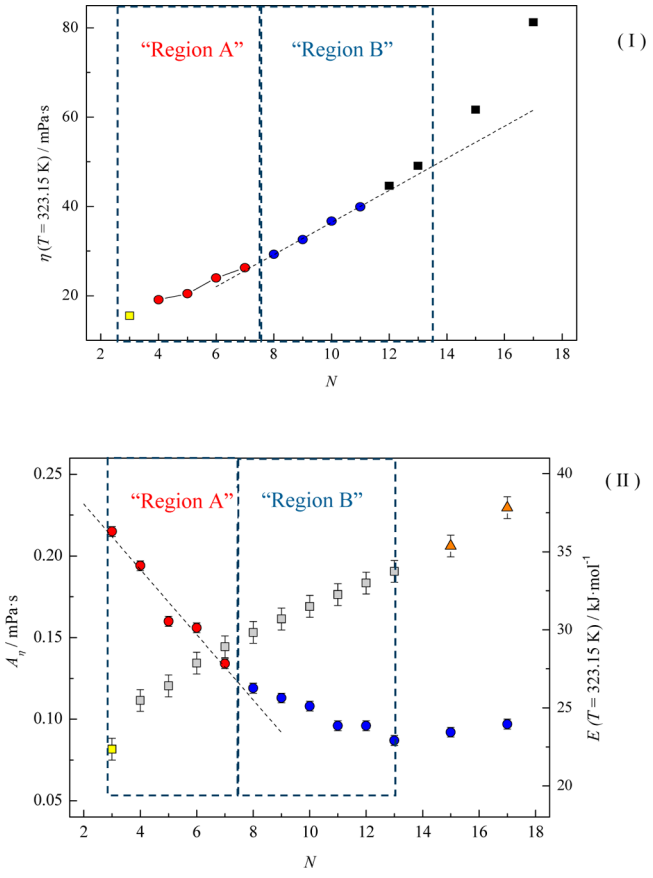

Figure 3. Plots of (I) viscosity (η/mPa·s) at T = 323.15 K and 0.1 MPa and (II) pre-exponential coefficient of the Vogel−Tammann−Fulcher equation (A_η/mPa·s) and energy barrier (E/kJ·mol^{-1}) at T = 323.15 K as a function of the total number of carbon atoms in the alkyl side chains of the cation, N, for the $[C_{N-1}C_1im][NTf_2]$ ionic liquid series. Yellow open squares and gray filled squares, E/kJ·mol^{-1}; red filled circles and blue filled circles, A_η/mPa·s.

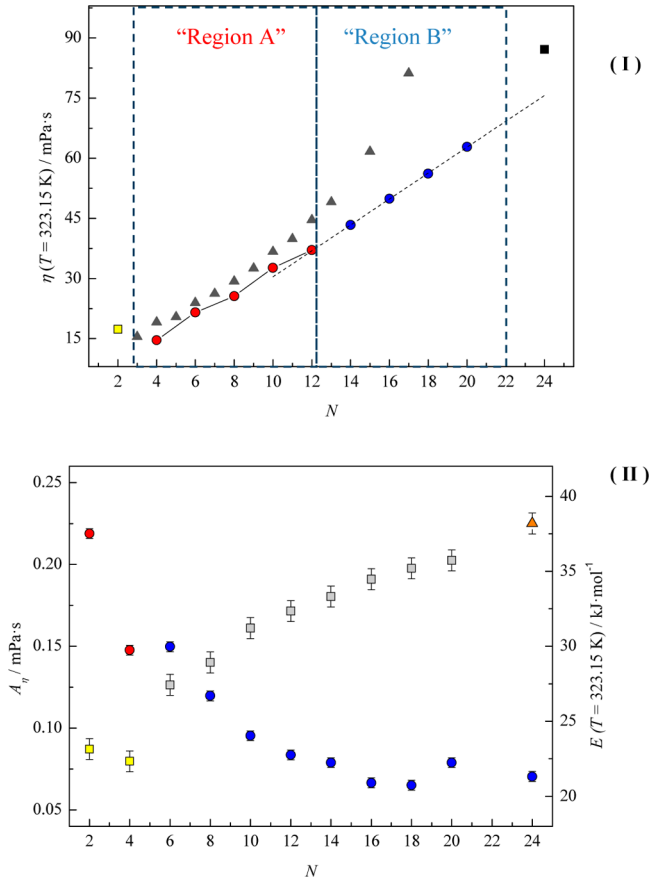

Figure 4. (I) Plots of $\eta(T$=323.15 K) = $f(N)$ for (yellow filled square, red filled circles, blue filled circles, black filled square) $[C_{N/2}C_{N/2}im][NTf_2]$and (gray filled triangles) $[C_{N-1}C_1im][NTf_2]$. (II) Graphic representation of the pre-exponential coefficient of the Vogel−Tammann−Fulcher equation (A_η/mPa·s) and energy barrier (E/kJ·mol^{-1}) at T = 323.15 K as a function of the total number of carbon atoms in the alkyl side chains of the cation, N, for $[C_{N/2}C_{N/2}im][NTf_2]$ ionic liquid family. Yellow filled squares and gray filled squares, E/kJ·mol^{-1}; red filled circles and blue filled circles, A_η/mPa·s.

$[C_{N-1}C_1im][NTf_2]$ and $[C_{N/2}C_{N/2}im][NTf_2]$ and further relate them to the density and viscosity data. It should be remarked that data were also collected over a wider Q range, but here we mainly focus on the low Q portion of the data, which contains information on the mesoscopic structural organization in these materials. Similarly to other ionic liquids, the diffraction patterns below 2 Å^{-1} are characterized by three amorphous peaks. In the family of dialkylimidazolium bistriflamide ionic liquids, these diffraction peaks are centered at ca. 0.2−0.5 (peak I), 0.9 (peak II), and 1.35 (peak III) Å^{-1}, for $[C_5C_5im][NTf_2]$, $[C_{10}C_1im][NTf_2]$, and $[C_{10}C_{10}im][NTf_2]$.

Samples such as $[C_5C_5im][NTf_2]$ and $[C_{10}C_1im][NTf_2]$ are characterized by comparable values for N, but inspection of Figure 6 indicates that the positions of the lowest Q peak, Q_I, are substantially different ($Q_I([C_5C_5im][NTf_2]) \approx 0.54$ Å^{-1} while $Q_I([C_{10}C_1im][NTf_2]) \approx 0.28$ Å^{-1}); on the other hand, the comparison between the data sets from $[C_{10}C_1im][NTf_2]$ ($Q_I \approx 0.28$ Å^{-1}) and $[C_{10}C_{10}im][NTf_2]$ ($Q_I \approx 0.32$ Å^{-1}) indicates that the corresponding values for Q_I are quite similar. This evidence indicates that the mesoscopic spatial order in these materials is mainly determined by the longest alkyl chain, regardless of the cation symmetry.

While volumetric quantities depend mostly on the total number carbons in the alkyl chain (N), the parameter that plays a role in determining the mesoscopic structure is υ, the number of alkyl groups in the longest chain that is either $\upsilon = N - 1$ in the case of asymmetric cations or $\upsilon = N/2$ in the case of symmetric cations. The available diffraction data (both data from ID15 (Figure 5) and from ID02 (data not shown)) were analyzed as a combination of three components (namely Lorentzian functions) in the Q range from 0.1 to 1.7 Å^{-1} in order to determine the alkyl chain length dependence of the peak positions, Q_i (with i = I−III), and, through Bragg's law ($D_i = 2\pi/Q_i$), of the corresponding characteristic sizes. These latter parameters are reported in Figure 7. The reported structural parameters are in excellent agreement with the existing data sets from other studies (e.g., our previous report for a more limited number of samples and the recent report from Martinelli and co-workers[29] that explores the asymmetric cation series up to $[C_{16}C_1im][NTf_2]$, at 323 K).

The higher Q peak centered at ca. 1.4 Å^{-1} (Q_{III}) shows barely any dependence on both alkyl chain length and the cation's symmetry/asymmetry, and the characteristic size associated with it, D_{III}, corresponds to ca. 4.6 Å.

This correlation length is related to characteristic distances between first neighbor opposite ions, which tends to organize in order to optimize their reciprocal distance, e.g., by imidazolium−imidazolium stacking. The intermediate peak

dx.doi.org/10.1021/jp406374a | J. Phys. Chem. B 2013, 117, 10889−10897

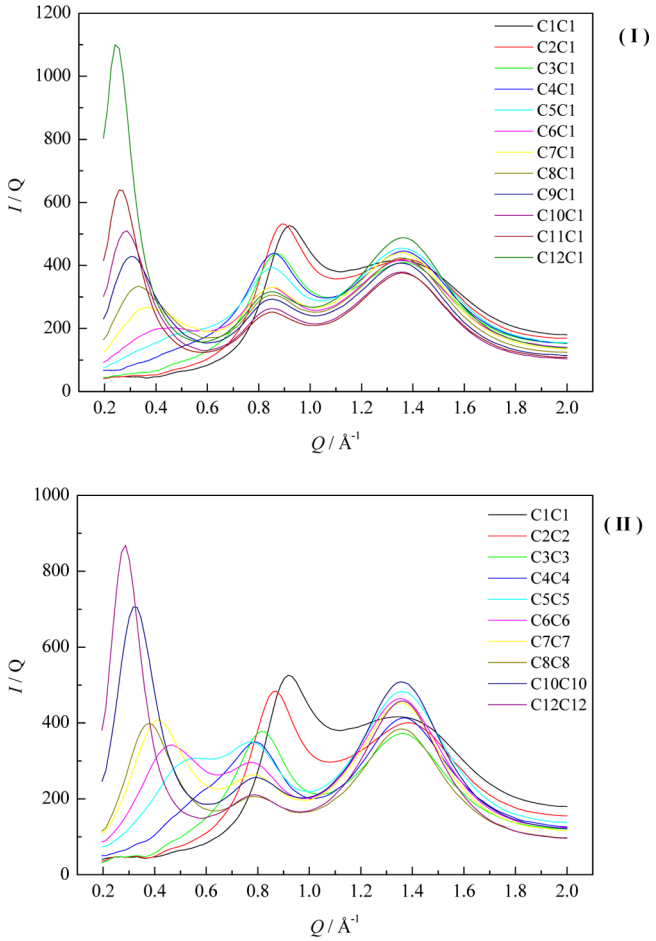

Figure 5. Comparison of SWAXS data for (I) $[C_{N-1}C_1im][NTf_2]$ (with N = 2−13) and (II) $[C_{N/2}C_{N/2}im][NTf_2]$ (with N = 2−16, 20, 24).

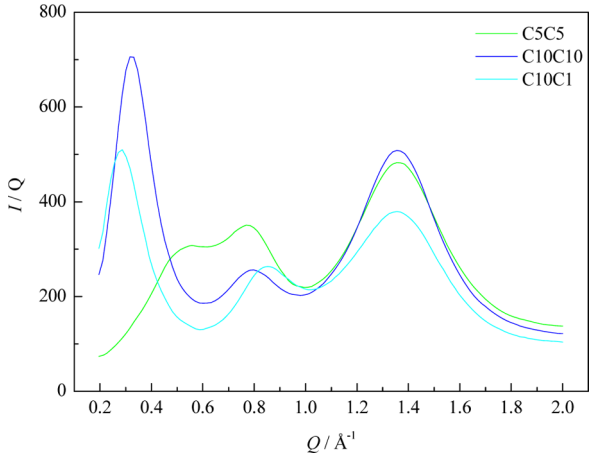

Figure 6. Comparison of SWAXS data for $[C_{10}C_1im][NTf_2]$, $[C_5C_5im][NTf_2]$, and $[C_{10}C_{10}im][NTf_2]$.

(Q_{II}) has a center at ca. 0.8 Å^{-1}. The position of this peak depends on the cation symmetry. The dependence from the alkyl chain length is negligible for $\upsilon \geq 6$, while it shifts substantially when increasing υ from 2 to 6. In particular in the case of dimethyl (υ = 1) D_{II} = 6.8 Å and upon increasing υ, D_{II} increases as well, reaching a plateau level at υ = 6, where D_{II} = 7.5 or 8.1 Å, for the case of asymmetric and symmetric cations,

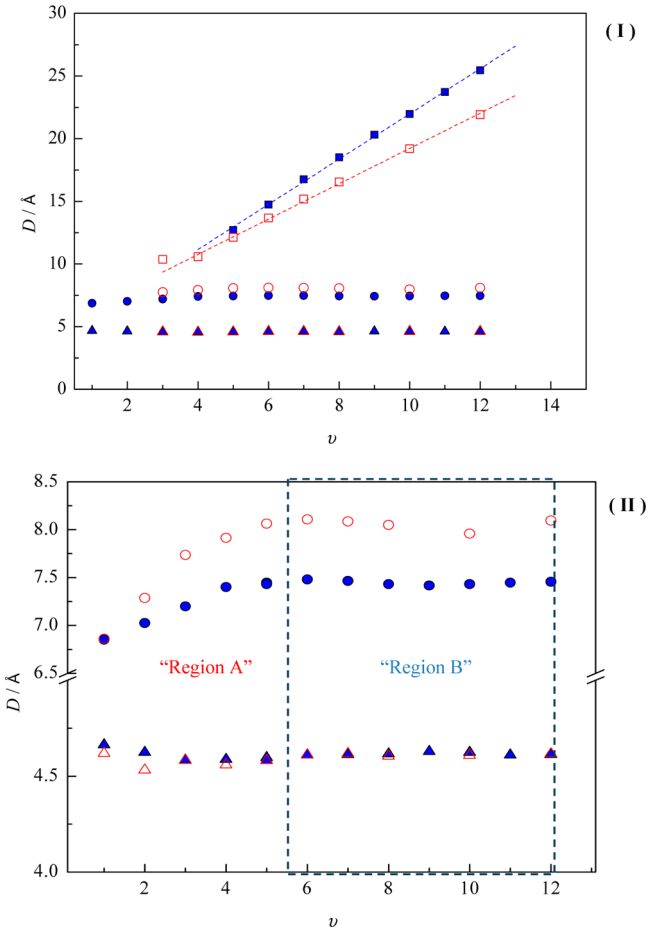

Figure 7. Alkyl chain length dependence of the characteristic size of nanoscale heterogeneities as obtained from the low Q peak position from SWAXS data for $[C_{N-1}C_1im][NTf_2]$ (with $\upsilon = N - 1$ = 2−12): blue filled squares, D_I, $dD/d\upsilon$ = (1.80 ± 0.02)Å; blue filled circles, D_{II}; blue filled triangles, D_{III}. Alkyl chain length dependence of the characteristic size of nanoscale heterogeneities as obtained from the low Q peak position from SWAXS data for $[C_{N/2}C_{N/2}im][NTf_2]$ (with $\upsilon = N/2$ = 1−8, 10, 12): red open squares, D_I, $dD/d\upsilon$ = (1.42 ± 0.02)Å; red open circles, D_{II}; red open triangles, D_{III}. υ, number of alkyl groups in the longest chain that is either $\upsilon = N - 1$ in the case of asymmetric or $\upsilon = N/2$ in the case of symmetric.

respectively. This spatial correlation length is related to the distance at which the closest ions of the same charge occur in the liquid. It is clear that above a threshold (υ = 6) this distance is no longer affected by the increasing of the alkyl chain length. These results are in agreement with the thermodynamic study concerning the vaporization of an extended series of ILs, $[C_{N-1}C_1im][NTf_2]$,[10,11] and with the viscosity data presented in this work, where two regions of different behaviors were found and a trend shift along the studied series was observed at $[C_6C_1im][NTf_2]$. Furthermore, it is noteworthy that a systematic difference of approximately 0.6 Å exists between these separations in the cases of symmetric and asymmetric cations. Presumably the steric hindrance stemming from the chains connected to the symmetric cations tends to separate the stacked imidazolium rings more than in the case of asymmetric cations. This may explain the slightly lower densities observed for the symmetric cations and is also in agreement with our recent work,[17] where a lower enthalpy of vaporization was found for the symmetric series $[C_{N/2}C_{N/2}im][NTf_2]$. The low

dx.doi.org/10.1021/jp406374a | J. Phys. Chem. B 2013, 117, 10889−10897

Q peak (Q_I) is centered at positions highly depending both on the cation symmetry and on the alkyl chain length. It can be appreciated that its detection is difficult for chains that are shorter than $\upsilon = 6$: in this range, it is both very broad and covered by the intermediate Q_{II} peak. Similarly to what has been reported in the past, the asymmetric series shows a linear trend for D vs υ.

A similar trend is here observed for the symmetric series over the whole accessible υ values. However, the characteristic slope for the two trends is substantially different well above the experimental uncertainties: namely, we find that the slopes $dD_I/d\upsilon$ are 1.80 ± 0.02 and 1.42 ± 0.02 Å per $-CH_2-$ unit for the asymmetric and symmetric cases, respectively. The large difference between these slopes indicates that the difference between D_I values for the symmetric and asymmetric series increases with increasing υ. This observation is at odds with the behavior found for the case of D_{II}, where the difference was maintained constant to ca. 0.6 Å for $\upsilon \geq 6$. Presumably these values for the slopes $dD_I/d\upsilon$ witness a different structural organization of the different classes of ILs. Wasserscheid and co-workers recently explored long chain symmetric imidazolium cation ILs, such as $[C_{12}C_{12}im][BF_4]$.[26]

In their report, they explore the crystalline structure of this class of ILs and find that the cations are organized in a rod shape with the two alkyl chains being stretched outward along the imidazolium plane, with the imidazolium/anion pair forming hydrophilic stacks and the long alkyl chains strongly interdigitating. This description of the crystalline phase of symmetric cation ILs is consistent with our present observation for the liquid state, as the value that we found for $dD_I/d\upsilon$ in the symmetric cation case is close to what one expects for full interdigitation (that corresponds to the $-CH_2-$ unit van der Waals diameter and equals ca. 1.27 Å per $-CH_2-$ unit). We already reported, including the case of bistriflamide anion, that asymmetric imidazolium cations are characterized by values for $dD_I/d\upsilon$ substantially larger than the $-CH_2-$ van der Waals diameter, thus indicating a poor interdigitation of the alkyl tails.[30,31]

The SWAXS technique probes merely structural effects and might be unable to detect purely dynamic effects that might affect the rheological measurements. We stress, however, that in a recent work[29] it was detected the existence of a nonnegligible deviation from linearity in the D vs υ trend plotted in Figure 7, for the alkyl chain length higher than $\upsilon > 12$, $[C_{12}C_1im][NTf_2]$. These measurements had been performed at higher temperatures (than room temperature); thus our data set probably is too limited to probe the existence of such a regime, which presumably is related to the higher conformational disorder in long alkyl chains. Such different structural conditions probably affect the viscosity of the corresponding ionic liquids.

4. CONCLUSIONS

The impact of the cation symmetry on the properties of imidazolium-based ionic liquid densities and viscosities as a function of temperature and small−wide angle X-ray scattering (SWAXS) patterns were evaluated for 1-alkyl-3-methylimidazolium bis(trifluoromethylsulfonyl)imide (asymmetric), $[C_{N-1}C_1im][NTf_2]$, and 1,3-dialkylimidazolium bis(trifluoromethylsulfonyl)imide (symmetric), $[C_{N/2}C_{N/2}im][NTf_2]$, series of ionic liquids. Above $N = 6$, the symmetric $[C_{N/2}C_{N/2}im][NTf_2]$ series presents a slightly lower density and lower viscosities than the asymmetric $[C_{N-1}C_1im][NTf_2]$ counterparts have. From $[C_2C_2im][NTf_2]$ to $[C_6C_6im][NTf_2]$, an odd−even effect was found in the viscosity along the alkyl side chain that vanishes in "Region B" where the structural segregation in ILs starts. A deviation toward higher viscosities for the long alkyl side chain ionic liquids was identified that could be related to the increase of the conformational entropy and possibility of alkyl chain folding, in agreement with the observed higher energy barriers arising from the increase of shear stress, identical to that observed for the long chain alkane derivatives.[27,28] Those observations were further supported by the small−wide angle X-ray scattering (SWAXS) pattern results. With reference to the observation of different chain length regimes in the density and viscosity determinations, it was observed that the SWAXS technique allows the detection of a major transition at $[C_5C_5im][NTf_2]$ for the symmetric series or at $[C_5C_1im][NTf_2]$ for the asymmetry series, where the low Q peak (Q_I) grows in a discernible way and the intermediate peak (Q_{II}) reaches a plateau level at $\upsilon = 6$. This threshold could be related to the development of well-established clusters stemming from the segregation of long enough alkyl tails in "Region B". This work highlights and gives an additional understanding of the change in the structural organization of ionic liquids above a critical alkyl length size (CALS).

■ ASSOCIATED CONTENT

Supporting Information

Experimental density and viscosity results at 0.1 MPa for the $[C_{N-1}C_1im][NTf_2]$ and $[C_{N/2}C_{N/2}im][NTf_2]$ ionic liquid series as a function of temperature. This material is available free of charge via the Internet at http://pubs.acs.org.

■ AUTHOR INFORMATION

Corresponding Authors

*E-mail: lbsantos@fc.up.pt.
*E-mail: jcoutinho@ua.pt.

Author Contributions

The manuscript was written through contributions of all authors. All authors have given approval to the final version of the manuscript. All authors contributed equally.

Notes

The authors declare no competing financial interest.

■ ACKNOWLEDGMENTS

This work was financed by national funding from FCT—Fundação para a Ciência e a Tecnologia, through the projects Pest-C/QUI/UI0081/2011, Pest-C/CTM/LA0011/2011, and PTDC/AAC-AMB/119172/2010. The authors also thank FCT for the Ph.D. and postdoctoral grants SFRH/BD/70641/2010, SFRH/BD/60513/2009, and SFRH/BPD/41781/2007 for C.M.S.S.N., M.A.A.R., and M.G.F., respectively. We acknowledge the European Synchrotron Radiation Facility for provision of synchrotron radiation facilities, and we would like to thank Dr. T. Narayanan and Dr. M. Di Michiel for assistance in using beamline ID02 and ID15b. A.T. acknowledges financial support from FIRB-Futuro in Ricerca (RBFR086BOQ) and PRIN (2009WHPHRH).

■ REFERENCES

(1) *Ionic Liquids in Synthesis*; Wasserscheid, P., Welton, T., Eds.; Wiley-VCH: Weinheim, Germany, 2003.

(2) Plechkova, N. V.; Seddon, K. R. In *Methods and Reagents for Green Chemistry: An Introduction*; Tundo, P., Perosa, A., Zecchini, F., Eds.; John Wiley & Sons, Inc.: New York, 2007; pp 105−130.
(3) Urahata, S. M.; Ribeiro, M. C. C. *J. Chem. Phys.* **2004**, *120*, 1855.
(4) Wang, Y.; Voth, G. A. *J. Am. Chem. Soc.* **2005**, *127*, 12192.
(5) Tokuda, H.; Ishii, K.; Susan, M. A. B. H.; Watanabe, M. *J. Phys. Chem. B* **2005**, *109*, 6103.
(6) Triolo, A.; Russina, O.; Bleif, H.-J.; Di Cola, E. *J. Phys. Chem. B* **2007**, *111*, 4641.
(7) Russina, O.; Triolo, A.; Gontrani, L.; Caminiti, R.; Xiao, D.; Hines, L. G., Jr.; Bartsch, R. A.; Quitevis, E. L.; Plechkova, N.; Seddon, K. R. *J. Phys.: Condens. Matter* **2009**, *21*, 424121.
(8) Pádua, A. A. H.; Canongia Lopes, J. N. *J. Phys. Chem. B* **2006**, *110*, 3330.
(9) Shimizu, K.; Costa Gomes, M. F.; Pádua, A. A. H.; Rebelo, L. P. N.; Canongia Lopes, J. N. *J. Mol. Struct.: THEOCHEM* **2010**, *946*, 70.
(10) Rocha, M. A. A.; Lima, C. F. R. A. C.; Gomes, L. R.; Schröder, B.; Coutinho, J. A. P.; Marrucho, I. M.; Esperança, J. M. S. S.; Rebelo, L. P. N.; Shimizu, K.; Canongia Lopes, J. N.; Santos, L. M. N. B. F. *J. Phys. Chem. B* **2011**, *115*, 10919.
(11) Rocha, M. A. A.; Bastos, M.; Coutinho, J. A. P.; Santos, L. M. N. B. F. *J. Chem. Thermodyn.* **2012**, *53*, 140.
(12) Dzyuba, S. V.; Bartsch, R. A. *Chem. Commun.* **2001**, 1466.
(13) Xiao, D.; Hines, L. G., Jr.; Li, S.; Bartsch, R. A.; Quitevis, E. L.; Russina, O.; Triolo, A. *J. Phys. Chem. B* **2009**, *113*, 6426.
(14) Zheng, W.; Mohammed, A.; Hines, L. G., Jr.; Xiao, D.; Martinez, O. J.; Bartsch, R. A.; Simon, S. L.; Russina, O.; Triolo, A.; Quitevis, E. L. *J. Phys. Chem. B* **2011**, *115*, 6572.
(15) Raju, S. G.; Balasubramanian, S. *J. Phys. Chem. B* **2010**, *114*, 6455.
(16) Raju, S. G.; Balasubramanian, S. *J. Mater. Chem.* **2009**, *19*, 4343.
(17) Rocha, M. A. A.; Coutinho, J. A. P.; Santos, L. M. N. B. F. *J. Phys. Chem. B* **2012**, *116*, 10922.
(18) Tariq, M.; Forte, P. A. S.; Costa Gomes, M. F.; Canongia Lopes, J. N.; Rebelo, L. P. N. *J. Chem. Thermodyn.* **2009**, *41*, 790.
(19) Tariq, M.; Carvalho, P. J.; Coutinho, J. A. P.; Marrucho, I. M.; Canongia Lopes, J. N.; Rebelo, L. P. N. *Fluid Phase Equilib.* **2011**, *301*, 22.
(20) Carvalho, P. J.; Regueira, T.; Santos, L. M. N. B. F.; Fernandez, J.; Coutinho, J. A. P. *J. Chem. Eng. Data* **2010**, *55*, 645.
(21) Tariq, M.; Serro, A. P.; Mata, J. L.; Saramago, B.; Esperança, J. M. S. S.; Canongia Lopes, J. N.; Rebelo, L. P. N. *Fluid Phase Equilib.* **2010**, *294*, 131.
(22) Jacquemin, J.; Husson, P.; Padua, A. A. H.; Majer, V. *Green Chem.* **2006**, *8*, 172.
(23) Tokuda, H.; Hayamizu, K.; Ishii, K.; Susan, M. A. B. H.; Watanabe, M. *J. Phys. Chem. B* **2005**, *108*, 16593.
(24) Costa Gomes, M. F.; Pison, L.; Pensado, A. S.; Padua, A. A. H. *Faraday Discuss.* **2012**, *154*, 41.
(25) Hasse, B.; Lehmann, J.; Assenbaum, D.; Wasserscheid, P.; Leipertz, A.; Fröba, A. P. *J. Chem. Eng. Data* **2009**, *54*, 2576.
(26) Wang, X.; Heinemann, F. W.; Yang, M.; Melcher, B. U.; Fekete, M.; Mudring, A. V.; Wasserscheid, P.; Meyer, K. *Chem. Commun.* **2009**, 7405.
(27) Queimada, A. J.; Stenby, E. H.; Marrucho, I. M.; Coutinho, J. A. P. *Fluid Phase Equilib.* **2003**, *212*, 303.
(28) Queimada, A. J.; Quiñones-Cisneros, S. E.; Marrucho, I. M.; Coutinho, J. A. P.; Stenby, E. H. *Int. J. Thermophys.* **2003**, *21*, 1221.
(29) Martinelli, A.; Maréchal, M.; Östlund, Å.; Cambedouzou, J. *Phys. Chem. Chem. Phys.* **2013**, *15*, 5510.
(30) Russina, O.; Triolo, A.; Gontrani, L.; Caminiti, R. *J. Phys. Chem. Lett.* **2012**, *3*, 27.
(31) Russina, O.; Triolo, A. *Faraday Discuss.* **2012**, *154*, 97.